Group Philicity and Electrophilicity as Possible Descriptors for Modeling Ecotoxicity Applied to Chlorophenols

ARTICLE *in* CHEMICAL RESEARCH IN TOXICOLOGY · APRIL 2006

Impact Factor: 3.53 · DOI: 10.1021/tx050322m · Source: PubMed

4 AUTHORS, INCLUDING:

R. Parthasarathi
Joint BioEnergy Institute
93 PUBLICATIONS **2,348** CITATIONS

Group Philicity and Electrophilicity as Possible Descriptors for Modeling Ecotoxicity Applied to Chlorophenols

J. Padmanabhan,[†] R. Parthasarathi,[†] V. Subramanian,*[,†] and P. K. Chattaraj*[,‡]

Chemical Laboratory, Central Leather Research Institute, Adyar, Chennai 600020, and Department of Chemistry, Indian Institute of Technology, Kharagpur 721302, India

Received November 17, 2005

The search for the best quantitative structure−activity relationship (QSAR) models in ecotoxicology is an ever-topical research activity. Hence, the development of new descriptors and applying them successfully in QSAR studies seems demanding in ecotoxicology. In the present work, group philicities are utilized for the first time in QSAR analysis for ecotoxicological studies on chlorophenols (CPs). It is important to point out that group philicities are capable of providing the best QSAR model for the toxicity of CPs against *Daphnia magna*. Furthermore, global electrophilicity and group philicities together give the best QSAR models for *Brachydanio rerio* and *Bacillus* with the maximum value of coefficient of determination and high internal predictive ability. The developed QSAR models clearly show the importance of the selected density functional reactivity indices as descriptors in ecotoxicological studies.

Introduction

Chlorophenols (CPs),[1] from mono- to pentachlorine-substituted compounds, are widely used either as synthetic intermediates in dyestuffs and pesticides or as biocides themselves. They occur as industrial wastes and direct pollutants in the environment and are relatively soluble in water and detectable in rivers, ponds, and soil (*1*). They can also be produced by environmental degradation of more complex molecules such as phenoxyacetic acids and chlorobenzenes. Thus, it is necessary to evaluate the hazards on nontarget organisms in the environment.

Among various organic water pollutants, phenol and its derivatives are supposed to be the most toxic as they are carcinogenic in nature (*2*, *3*). Phenols have been reported to have a matrixectomy effect on diabetic patients (*4*). The adverse effects of phenolic compounds have also been found on some useful bacteria (nitrification bacteria, bacteria in sediment, etc.) in nature (*5*, *6*). It is very interesting to observe that many phenolic compounds are present in wastewaters of paper and pulp, pesticides, dyes, textiles, pharmaceutical, plastic, rubber, tanning, and petroleum industries (*7*). Phenols are also present in domestic effluents and vegetation decay. Therefore, the toxicity of phenol and its derivatives even at a trace level attracted scientists to develop suitable technology for their removal from water.

Quantitative structure−activity relationship (QSAR) methods can be applied for the prediction of biological activity from chemical structures or properties. From an environmental standpoint, the types of activity that can be estimated by QSARs include aquatic toxicity and biodegradability. For some chemical species, QSAR modeling is a useful technique to correlate their physical, chemical, biological, or environmental activities to their physicochemical property descriptors. Because the experimental determination is time-consuming and expensive, estimated values based on QSAR models are now widely used.

The research and development of QSAR models in ecotoxicology are, more than ever, topical. Indeed, interest is very strong, especially in the context of regulation of industrial chemicals. As a general rule, legislation allows the use of QSAR and several countries including the United States use them widely (*8*). These observations prompted the search for new QSAR tools and therefore the study of applications of molecular modeling methods, from pharmaceutical sciences to ecotoxicology. Several methods such as comparative molecular field analysis (CoMFA) (*9*) and the free energies of solvation with continuum models on CPs have been investigated (*10*).

The toxicity of CPs increases with an increase in the number of chlorine atoms and gets reduced by the chlorine atoms substituted at the ortho-position (*11*). Kishino et al. (*12*) while analyzing the relation between the acute toxicity of CPs in fish and their chemical structures have found that the toxicity of CPs increases with an increasing number of chlorine atoms, and the toxicity of CPs having the same number of chlorine atoms decreases in the order of non-, mono-, and di-*ortho*-CPs.

Conceptual density functional theory (DFT) has been successfully exploited to unravel chemical reactivity and site selectivity (*13*−*15*). Recently, our group has carried out reactivity/toxicity analysis on PCBs and other systems using DFT-based descriptors (*16*−*22*). Because the transfer of electrons (or a nucleophile in a general sense) between a toxin and a receptor is the crux of the toxicity, electron affinity, planarity, and electrophilicity have turned out to be natural descriptors of the toxic nature of these compounds (*19*, *20*). In the present study, the experimental ecotoxicological data of CPs chosen for QSAR analysis are as follows: (i) EC_{50} on *Daphnia magna*, effective concentrations causing 50% immobilization of daphniae after 24 h of exposure (*23*); (ii) LC_{50} on *Brachydanio rerio*, lethal concentrations for 50% of fish after 24 h of exposure (*23*, *24*); and (iii) IC_{50} on *Bacillus* sp. TL81, effective

* To whom correspondence should be addressed. (V.S.) Tel: +91-44-24411630. Fax: +91-44-24911589. E-mail: subuchem@hotmail.com. (P.K.C.) E-mail: pkc@chem.iitkgp.ernet.in.

[†] Central Leather Research Institute.

[‡] Indian Institute of Technology.

[1] Abbreviations: CPs, chlorophenols; QSAR, quantitative structure−activity relationships; CoMFA, comparative molecular field analysis; DFT, density functional theory; LOO, leave-one-out; MCP, monochlorophenol; DCP, dichlorophenol; TCP, trichlorophenol; TTP, tetrachlorophenol; PCP, pentachlorophenol; AHH, aryl hydrocarbon hydroxylase; NIMAG, number of imaginary frequencies.

10.1021/tx050322m CCC: $33.50
Published on Web 02/10/2006

concentrations of the toxicant causing 50% inhibition of the bacterial dehydrogenase activity (*25*, *26*). The QSAR models are built with above-said experimental toxicity data as dependent variables and group philicities (ω_g^+, ω_g^-) and/or global electrophilicity (ω) as independent variables for the series of CPs.

Theoretical Background

According to DFT (*27*, *28*), the chemical potential (μ) and chemical hardness (η) are defined as

$$\chi = -\mu = -\left(\frac{\partial E}{\partial N}\right)_{v(\vec{r})} \tag{1}$$

and

$$\eta = \frac{1}{2}\left(\frac{\partial^2 E}{\partial N^2}\right)_{v(\vec{r})} = \frac{1}{2}\left(\frac{\partial \mu}{\partial N}\right)_{v(\vec{r})} \tag{2}$$

where E is the total energy of the system, N is the number of electrons in the system, and $v(\vec{r})$ is the external potential. μ is identified as the negative of the electronegativity (χ) as defined by Iczkowski and Margrave (*29*).

To save the computational time, we have calculated chemical potential and chemical hardness by using Koopmans' theorem (*27*) as

$$\mu = \frac{E_{\mathrm{LUMO}} + E_{\mathrm{HOMO}}}{2} \tag{3}$$

and

$$\eta = \frac{E_{\mathrm{LUMO}} - E_{\mathrm{HOMO}}}{2} \tag{4}$$

where E_{LUMO} is the lowest unoccupied molecular orbital's energy and E_{HOMO} is the highest occupied molecular orbital's energy.

The Fukui function, which measures the sensitivity of a system's chemical potential to an external perturbation at a particular site, is defined as (*28*)

$$f(\vec{r}) = \left(\frac{\partial \rho(\vec{r})}{\partial N}\right)_{v(\vec{r})} = \left(\frac{\delta \mu}{\delta v(\vec{r})}\right)_N \tag{5}$$

Because the above derivatives are discontinuous, three different types of Fukui functions have been defined (*30*−*32*)

$$f^+(\vec{r}) = \rho_{N+1}(\vec{r}) - \rho_N(\vec{r}) \text{ for nucleophilic attack} \tag{6a}$$

$$f^-(\vec{r}) = \rho_N(\vec{r}) - \rho_{N-1}(\vec{r}) \text{ for electrophilic attack} \tag{6b}$$

$$f^0(\vec{r}) = [\rho_{N+1}(\vec{r}) - \rho_{N-1}(\vec{r})]/2 \text{ for radical attack} \tag{6c}$$

Parr et al. have introduced a global electrophilicity index ω as (*33*)

$$\omega = \frac{\mu^2}{2\eta} \tag{7}$$

According to this definition, ω measures the ability of a molecular species to soak up electrons and is used in understanding the reactivity of the human immunodeficiency virus type 1 (HIV-1) nucleocapsid protein p7 (NCp7) when reacted with a variety of electrophilic agents (*34*).

Recently, Chattaraj et al. (*35*) proposed a generalized concept of philicity containing electrophilic, nucleophilic, and radical reactions. The condensed-to-atom variants for the atomic site "*k*" have been written as

$$\omega_k^\alpha = \omega f_k^\alpha \tag{8}$$

where $\alpha = +, -$, and 0 refer to nucleophilic, electrophilic, and radical attacks, respectively. The ω_k^α will vary from atom to atom in a molecule, but the sum of any ω_k^α over all atoms is conserved.

The condensed philicity summed over a group of relevant atoms is defined as the "group philicity". It can be expressed as (*36*)

$$\omega_g^\alpha = \sum_{k=1}^{n} \omega_k^\alpha \tag{9}$$

where n is the number of atoms coordinated to the reactive atom, ω_k^α is the local philicity of the atom k, ω_g^α is the group philicity obtained by adding the local philicity of the nearby bonded atoms, and $\alpha = +, -, 0$ represents nucleophilic, electrophilic, and radical attacks, respectively.

The global interactions between the constituents of CPs and nucleic acid (NA) bases/aryl hydrocarbon hydroxylase (AHH) receptors such as histidine, phenylalanine, and tryptophan have been determined using the parameter ΔN, which represents the fractional number of electrons, transferred from system A to system B, and is represented by (*37*)

$$\Delta N = \frac{\mu_B - \mu_A}{2(\eta_A + \eta_B)} \tag{10}$$

where μ_A, μ_B and η_A, η_B are the chemical potentials and chemical hardnesses of systems A and B, respectively.

Methods for Data Analysis

The set of 18 CPs considered in this study is divided into two groups, namely, the training set and the test set. The test set consists of 10% (two CPs) of the entire set of 18 CPs, and the training set contains the remaining 16 CPs. Initially, linear/multilinear regression analyses are performed using experimental toxicity values as dependent variables and various combinations of the selected descriptors as independent variables on the training set. Internal validations of the model for the training set have been performed using cross-validation (*38*, *39*). In cross-validation, a model is calculated with groups of object (CPs) omitted subsequently, followed by the prediction of the target property for the omitted objects. In the present study, the leave-one-out (LOO) method is adopted and the procedure is repeated until all of the objects have been omitted once. Internal predictability of the models is characterized by the cross-validated squared correlation coefficient (r_{cv}^2) given by

$$r_{cv}^2 = 1 - \frac{\sum_i (Y_i^{\mathrm{pred}} - Y_i^{\mathrm{obs}})^2}{\sum_i (Y_i^{\mathrm{obs}} - Y^{\mathrm{mean}})^2} \tag{11}$$

where Y_i^{obs}, Y_i^{pred}, Y^{mean} are, respectively, the observed, predicted, and the observed mean values of the dependent variables; the summations run over all compounds in the training set.

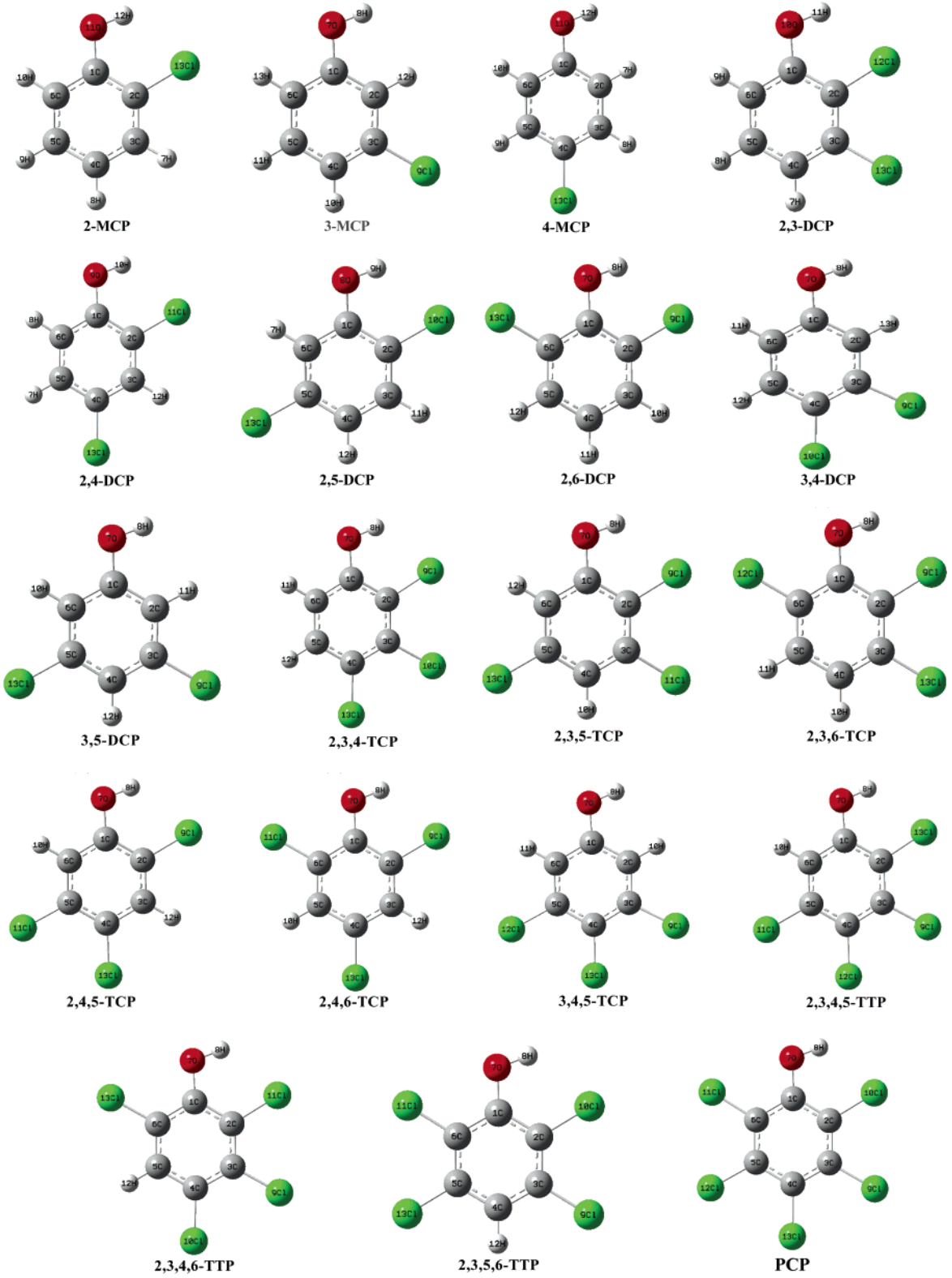

Figure 1. Structures along with atom numbering for the series of CPs.

The resulting best model using the training set has been chosen to predict the toxicity values of the CPs in the test set. Then, the training and test sets are combined and the above process of regression analysis and validation is carried out on this data set to select the best model for prediction.

Computational Details

The geometries of selected 19 CPs are optimized using Becke's three parameter hybrid density functional, B3LYP/6-31G*, which includes both Hartree−Fock exchange and DFT exchange correlation functionals (*40*−*42*) as implemented in the Gaussian 98W suite of programs (*43*). The optimized geometries are characterized by harmonic vibrational frequencies, which confirmed that the structures obtained are minimum on the potential energy surface since they are associated with zero NIMAG (number of imaginary frequencies) values. The global electrophilicity index (ω) is calculated using eq 7. Hirshfeld population scheme (Stockholder partitioning scheme)

Table 1. Calculated Conceptual Density Functional Reactivity Descriptors in a.u. for the Series of CPs from the B3LYP/6-31G* Method

molecule[a]	chemical potential (μ)	chemical hardness (η)	electrophilicity index (ω)	group philicity ω_g^+ (C_1OH)	group philicity ω_g^- (C_1OH)
2-MCP	−0.1213	0.1083	0.0680	0.0084	0.0183
3-MCP	−0.1223	0.1087	0.0688	0.0090	0.0174
4-MCP	−0.1193	0.1045	0.0681	0.0089	0.0174
2,3-DCP	−0.1314	0.1068	0.0808	0.0095	0.0207
2,4-DCP	−0.1306	0.1028	0.0829	0.0097	0.0200
2,5-DCP	−0.1330	0.1063	0.0832	0.0098	0.0175
2,6-DCP	−0.1317	0.1065	0.0815	0.0090	0.0201
3,4-DCP	−0.1293	0.1034	0.0808	0.0099	0.0187
3,5-DCP	−0.1352	0.1084	0.0843	0.0104	0.0212
2,3,4-TCP	−0.1376	0.1015	0.0932	0.0103	0.0212
2,3,5-TCP	−0.1425	0.1057	0.0961	0.0108	0.0203
2,3,6-TCP	−0.1396	0.1038	0.0939	0.0099	0.0181
2,4,5-TCP	−0.1394	0.1015	0.0957	0.0106	0.0202
2,4,6-TCP	−0.1400	0.1013	0.0967	0.0101	0.0220
3,4,5-TCP	−0.1387	0.1026	0.0938	0.0109	0.0208
2,3,4,5-TTP	−0.1460	0.1005	0.1061	0.0111	0.0220
2,3,4,6-TTP	−0.1458	0.0995	0.1068	0.0107	0.0215
2,3,5,6-TTP	−0.1484	0.1033	0.1066	0.0104	0.0198
PCP	−0.1518	0.0987	0.1167	0.0110	0.0231

[a] TTP, tetrachlorophenol.

(*44*) has been used to calculate Fukui function values as implemented in the DMOL^3 package (*45*) employing the BLYP/DND method. Local philicities (ω^+, ω^-) and, hence, group philicities (ω_g^+, ω_g^-) are calculated using eqs 8 and 9, respectively. Charge transfer between CPs and various nucleic acid bases/AHH receptors such as histidine, phenylalanine, and tryptophan is calculated using eq 10. One, two, and three parameter QSARs (*46*) are performed using least-squares error estimation method (*47*) to calculate the toxicity values.

Results and Discussion

Descriptors of CPs. The optimized structures of various CPs are depicted along with atom numbering (Figure 1). Table 1 lists the calculated values of chemical potential (μ), chemical hardness (η), electrophilicity index (ω), and group philicities (ω_g^+, ω_g^-) for the series of selected CPs. Group philicity is obtained by adding the local philicity of the relevant atoms, that is, nearby bonded atoms. In the present study, the functional group atoms (−OH) along with its nearby bonded atom (C_1 atom; Figure 1) are considered and their respective summed local philicities ($\sum\omega^+$ and $\sum\omega^-$) are taken as group philicities (ω_g^+, ω_g^- with g as C_1OH).

The values of ω clearly predict that with an increase in the number of chlorine substitution, the chemical reactivity of CPs increases (Figure 2). Hence, with the selected CPs, monochlorophenol (MCP) has minimum chemical reactivities and pentachlorophenol (PCP) has the maximum chemical reactivity. Also, it can be seen that ω_g^+ and ω_g^- show an increase in their values with an increase in the number of chlorine substitutions (Table 1). Because experimental ecotoxicity values for CPs also show an increase with the increase in the number of chlorine substitutions (see Tables 6, 9, and 12), selection of ω, ω_g^+, and ω_g^- as descriptors seems realistic.

Charge Transfer Analysis. The chemical potential (μ) and chemical hardness (η) for NA bases viz., adenine, guanine, thymine, cytosine, and uracil, and AHH receptors such as histidine, phenylalanine, and tryptophan, are presented in Table 2. If two systems X and Y are brought together, as in a reaction, they must form a single system with the constant values of chemical potential. The negative of the chemical potential can be called the absolute electronegativity, and there is always a transfer of electrons from less electronegative systems to more electronegative systems. The amounts of charge transfer between CPs and various nucleic acid bases/AHH receptors are calculated using eq 10 to know about the possible interaction of CPs with the biosystems (Table 3). Positive values in Table 3 indicate that the respective CPs act as electron acceptors, and negative values indicate that the corresponding CPs act as electron donors. With this idea, one can say that all selected CPs act as electron acceptors with adenine and guanine. With thymine, mono- and di-CPs act as electron donors and other CPs as electron acceptors. Also, mono-CPs act as electron donors with cytosine and other CPs as electron acceptors. In the case of interaction of CPs with uracil, all CPs other than tetra- and penta-CPs act as electron donors. In the interaction of CPs with the selected AHH receptors, all CPs act as electron acceptors with the exception of mono-CPs with histidine. Previous studies (*16*−*22*) have shown that for analyzing the reactivity of electron acceptors and electron donors, ω^+ and ω^- can be used, respectively. Because a mixed donor/acceptor characteristic is seen in the case of interaction of CPs with NA bases/AHH receptors, in the present study, both ω_g^+ and ω_g^- are utilized along with ω for the QSAR analysis.

This type of electron transfer mechanism in biosystems is not unknown. For example (*48*), the electron transfer flavoprotein:ubiquinone oxido reductase (ETFQO) is a component of a side chain of redox reactions, which help the electron transfer to the ubiquinone and accordingly to the electron transport chain. This electron transfer process gets catalyzed by oxidoreductase, and it occurs from the electron transfer flavoprotein (ETF) to ubiquinone through its prosthetic group and Fe−S center. In mammals, ETF accepts electrons from at least nine mitochondrial matrix flavoprotein dehydrogenases before transferring

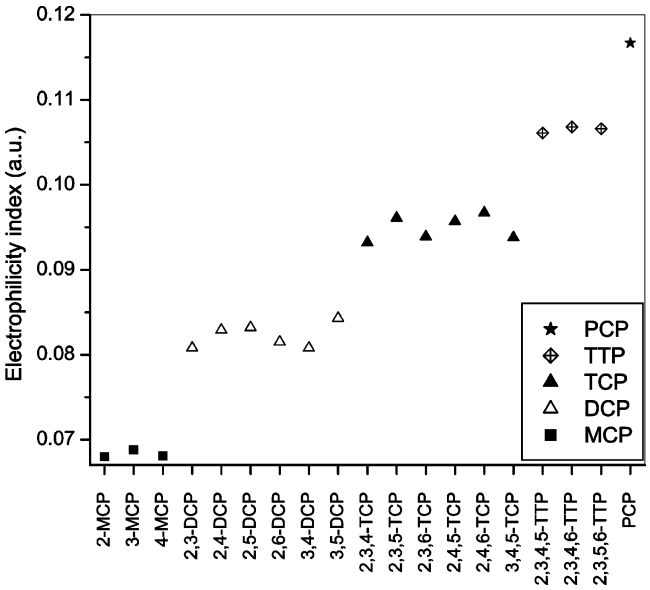

Figure 2. Variation of electrophilicity index with increasing chlorine substitution for different CPs.

Table 2. Calculated Chemical Potential (μ) and Chemical Hardness (η) for Nucleic Acid Bases/AHH Receptors from the B3LYP/6-31G* Method

molecule	μ (a.u.)	η (a.u.)	molecule	μ (a.u.)	η (a.u.)
adenine	−0.1140	0.1047	uracil	−0.1440	0.1089
thymine	−0.1356	0.1064	histidine	−0.1227	0.1099
guanine	−0.0973	0.1072	phenylalanine	−0.1077	0.0963
cytosine	−0.1238	0.1023	tryptophan	−0.1139	0.1047

Table 3. Calculated Charge Transfer between CPs and Nucleic Acid Bases/AHH Receptors from the B3LYP/6-31G* Method

molecule	adenine	thymine	guanine	cytosine	uracil	histidine	phenylalanine	tryptophan
2-MCP	0.0172	−0.0332	0.0558	−0.0059	−0.0522	−0.0031	0.0333	0.0174
3-MCP	0.0194	−0.0310	0.0579	−0.0036	−0.0499	−0.0010	0.0356	0.0196
4-MCP	0.0127	−0.0386	0.052	−0.0109	−0.0579	−0.0079	0.0289	0.0129
2,3-DCP	0.0412	−0.0098	0.0797	0.0182	−0.0292	0.0201	0.0584	0.0414
2,4-DCP	0.0399	−0.0120	0.0792	0.0165	−0.0317	0.0185	0.0574	0.0402
2,5-DCP	0.0450	−0.0061	0.0836	0.0221	−0.0256	0.0238	0.0624	0.0453
2,6-DCP	0.0420	−0.0090	0.0806	0.0190	−0.0284	0.0209	0.0593	0.0423
3,4-DCP	0.0367	−0.0151	0.0759	0.0133	−0.0347	0.0154	0.0540	0.0370
3,5-DCP	0.0497	−0.0010	0.0878	0.0270	−0.0203	0.0286	0.0671	0.0499
2,3,4-TCP	0.0571	0.0047	0.0964	0.0338	−0.0153	0.0351	0.0755	0.0574
2,3,5-TCP	0.0678	0.0164	0.1063	0.0451	−0.0034	0.0460	0.0863	0.0681
2,3,6-TCP	0.0615	0.0096	0.1003	0.0384	−0.0103	0.0396	0.0798	0.0617
2,4,5-TCP	0.0615	0.0090	0.1007	0.0382	−0.0111	0.0394	0.0800	0.0617
2,4,6-TCP	0.0632	0.0107	0.1024	0.0398	−0.0094	0.0410	0.0818	0.0634
3,4,5-TCP	0.0596	0.0075	0.0987	0.0364	−0.0125	0.0377	0.0780	0.0599
2,3,4,5-TTP	0.0780	0.0252	0.1173	0.0548	0.0048	0.0554	0.0973	0.0783
2,3,4,6-TTP	0.0779	0.0248	0.1174	0.0546	0.0044	0.0552	0.0974	0.0782
2,3,5,6-TTP	0.0826	0.0305	0.1213	0.0598	0.0103	0.0602	0.1019	0.0829
PCP	0.0929	0.0395	0.1323	0.0696	0.0188	0.0697	0.1131	0.0932

Table 4. Regression Models for the Toxicity [log(1/EC$_{50}$)] against *D. magna* Using Various Descriptors for a Training Set of 16 CPs

s. no.	regression equation	r^2	r_{cv}^2	SD
1	$\log(1/EC_{50}) = -2.2 + 198.0 \times \omega_g^-$	0.515	0.374	0.348
2	$\log(1/EC_{50}) = -0.9 + 28.7 \times \omega$	0.731	0.671	0.259
3	$\log(1/EC_{50}) = -1.4 + 24.8 \times \omega + 42.0 \times \omega_g^-$	0.741	0.630	0.264
4	$\log(1/EC_{50}) = -3.8 + 545.6 \times \omega_g^+$	0.874	0.835	0.177
5	$\log(1/EC_{50}) = -3.5 + 3.5 \times \omega + 491.3 \times \omega_g^+$	0.877	0.802	0.813
6	$\log(1/EC_{50}) = -4 - 0.6 \times \omega + 492.3 \times \omega_g^+ + 43.26 \times \omega_g^-$	0.887	0.792	0.182
7	$\log(1/EC_{50}) = -4.0 + 485.3 \times \omega_g^+ + 41.9 \times \omega_g^-$	0.887	0.826	0.175

Table 5. Regression Models for the Toxicity [log(1/EC$_{50}$)] against *D. magna* Using Various Descriptors for the Data Set of 18 CPs

s. no.	regression equation	r^2	r_{cv}^2	SD
1	$\log(1/EC_{50}) = -2.2 + 196.2 \times \omega_g^-$	0.529	0.409	0.326
2	$\log(1/EC_{50}) = -0.8 + 28.4 \times \omega$	0.704	0.644	0.260
3	$\log(1/EC_{50}) = -1.6 + 22.4 \times \omega + 65.5 \times \omega_g^-$	0.731	0.634	0.254
4	$\log(1/EC_{50}) = -3.8 + 546.5 \times \omega_g^+$	0.876	0.842	0.167
5	$\log(1/EC_{50}) = -3.6 + 3.3 \times \omega + 496.4 \times \omega_g^+$	0.879	0.817	0.171
6	$\log(1/EC_{50}) = -3.9 + 0.6 \times \omega + 477.3 \times \omega_g^+ + 40.2 \times \omega_g^-$	0.889	0.812	0.170
7	$\log(1/EC_{50}) = -4.0 + 484.6 \times \omega_g^+ + 41.4 \times \omega_g^-$	0.889	0.838	0.164

them to the ubiquinone in the inner mitochondrial membrane. In the case of mammals, this process is involved in the β-oxidation of fatty acids and catabolism of amino acids and choline and the deficiency of the oxido reductase (an autosomal recessive trait) causes glutaric aciduria, type II.

Several experimental investigations have been carried out in the literature (*49*−*53*) showing the interaction of CPs with DNA and proteins, which may possibly be taking place through charge transfer phenomena either directly or indirectly. CPs are classified as probable human carcinogens and are known to undergo bioactivation to generate benzoquinone (BQ) electrophiles that react covalently with biopolymers. Recently, Manderville et al. (*49*) characterized the ability of PCP to react covalently with deoxyguanosine (dG) following treatment with horseradish peroxidase (HRP)/H_2O_2 or myeloperoxidase to yield a C8-dG oxygen (O) adduct that suggested the intermediacy of the pentachlorophenoxyl radical in covalent bond formation. Also, investigations focused on a wider range of CP substrates [PCP, 2,4,6-TCP, 2,4,5-TCP, and 2,4-dichlorophenol (DCP)] to establish their reactivity toward dG and duplex DNA [calf thymus (CT)] following activation by HRP/H_2O_2, as a representative peroxidase system that has also been carried out (*50*). The data showed that chlorophenoxyl radicals may either react directly with dG and CT-DNA to form C8-dG O adducts in an irreversible process or couple to yield 1,4-BQ electrophiles that react with dG to afford adducts of the benzetheno variety. These results (*50*) are the first to establish the in vitro relevance of C8-dG O adducts of phenolic toxins. Overall, the results from the study have provided new insights into peroxidase-mediated activation of CP substrates and have strengthened the hypothesis that direct reactions of phenoxyl radicals with DNA contribute to peroxidase-driven toxic effects of phenolic xenobiotics.

In another study (*51*), primary cultured rat hepatocytes were used as an experimental model to detect adverse effects of five CPs in vitro (penta-CP, 2,3,4,5-tetra-CP, 2,4,5,-tri-CP, 2,4-di-CP, and 4-mono-CP). Monolayer cultures were exposed to the test compounds for 1 h, and concentration−response curves were established with respect to the effects on phase I and phase II metabolism of 7-ethoxycoumarin (7-EC) and on cellular ATP content. All CPs tested inhibited the O-dealkylation of 7-EC, with half-maximum effective concentrations (EC_{50}) ranging from about 36 μM for the three highest chlorinated phenols to 215 μM for 4-mono-CP, which proved to be least effective. The subsequent conjugation of the primary metabolite 7-hydroxycoumarin was even more sensitive toward CP exposure than the O-deethylation process. The concentrations that reduced the percentage of conjugated metabolite to 50% of the respective control cultures ranged from 7 μM for penta-CP to 48 μM for 4-mono-CP. Treatment of cultured hepatocytes with CP additionally resulted in a depletion of cellular ATP at EC_{50} concentrations ranging from 6 μM for penta-CP to 1330 μM for 4-mono-CP. Also, microsomal metabolism of PCP was investigated (*52*), with special attention to the conversion-dependent covalent binding to protein and DNA. It has been shown that PCP metabolism leads to the production of multiple adducts arising from both tetrachloro-1,2-benzoquinone (Cl_4-

Table 6. Experimental and Calculated Values of Toxicity [log(1/EC_{50})] against *D. magna* for the Model Constructed Using the Data Set of 18 CPs

		log(1/EC_{50}) value (mmol/L)		
s. no.	molecule	experimental[a]	calculated[b]	residual[c]
1	2-MCP	0.85	0.83	0.02
2	3-MCP	0.91	1.08	−0.17
3	4-MCP	1.20	1.03	0.17
4	2,3-DCP	1.50	1.46	0.04
5	2,4-DCP	1.78	1.53	0.25
6	2,5-DCP	1.52	1.47	0.05
7	2,6-DCP	1.24	1.19	0.05
8	3,4-DCP	1.77	1.57	0.20
9	3,5-DCP	1.89	1.92	−0.03
10	2,3,4-TCP	1.94	1.87	0.07
11	2,3,5-TCP	1.94	2.07	−0.13
12	2,3,6-TCP	1.43	1.55	−0.12
13	2,4,5-TCP	1.98	1.97	0.01
14	2,4,6-TCP	1.56	1.81	−0.25
15	3,4,5-TCP	2.35	2.14	0.21
16	2,3,4,5-TTP	2.12	2.29	−0.17
17	2,3,4,6-TTP	-	2.08[d]	-
18	2,3,5,6-TTP	2.01	1.86	0.15
19	PCP	2.54	2.29	0.25

[a] Experimental data as obtained from ref *23*. [b] With ω_g^+ and ω_g^- as descriptors. [c] Difference between experimental and calculated toxicity values. [d] Predicted value using the developed model.

1,2-BQ) and tetrachloro-1,4-benzoquinone (Cl_4-1,4-BQ) in rats and mice (*53*).

QSAR Analysis. In this section, QSAR studies were carried out for analyzing the toxicity of CPs on three selected species, viz. *D. magna*, *B. rerio*, and *Bacillus*.

CP vs *D. magna*. The selected set of 18 CPs is divided into a training set (16 molecules) and a test set (two molecules). Linear regression analyses using experimental toxicity [log(1/EC_{50})] (*23*) against *D. magna* as a dependent variable and various combinations of the selected descriptors as independent variables are carried out on the training set (Table 4). It is the group philicity (ω_g^+ and ω_g^-) combination, which is capable of explaining maximum variation (88.7%) in data along with a high value for the cross-validated squared correlation coefficient (r_{cv}^2) of 0.826. Hence, this QSAR model is used to predict the log(1/EC_{50}) values of molecules in the test set. That is, for 3,5-DCP (2,3,4-TCP), the observed log(1/EC_{50}) value is 1.89 (1.94) and the predicted value is 1.94 (1.89).

Now, the training and test compounds are combined and the regression analysis is carried out on this combined data set (Table 5). Table 6 lists the observed and calculated values of log(1/EC_{50}) for CPs against *D. magna*. It is the group philicity (ω_g^+ and ω_g^-) combination, which is again capable of explaining maximum variation (88.9%) in data along with a high value for the cross-validated squared correlation coefficient (r_{cv}^2) of 0.838 and a low value for root-mean-square error, SD, of 0.164. A plot between observed and calculated values of log(1/EC_{50}) for CPs against *D. magna* (Figure 3A) shows a correlation coefficient, *r*, of 0.942.

CP vs *B. rerio*. Linear regression analyses using experimental toxicity [log(1/LC_{50})] (*23*, *24*) against *B. rerio* as a dependent variable and various combinations of the selected descriptors as independent variables are carried out on the training set of 16 CPs (Table 7). ω along with group philicities (ω_g^+ and ω_g^-) are capable of explaining maximum variation (93.1%) in data with a cross-validated squared correlation coefficient (r_{cv}^2) of 0.882. Hence, this QSAR model is used to predict the log(1/LC_{50}) values of molecules in the test set. That is, for 3,5-DCP (2,3,4-TCP), the observed log(1/LC_{50}) value is 1.97 (2.01) and the predicted value is 2.16 (2.03).

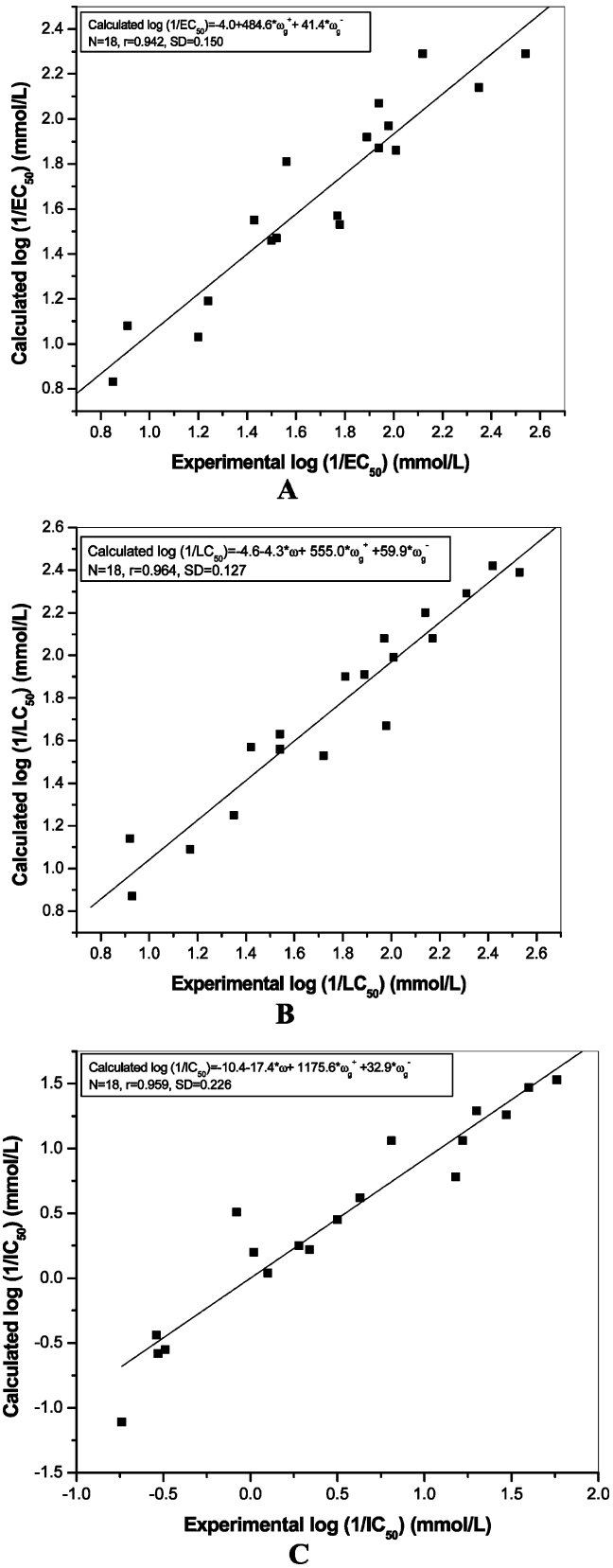

Figure 3. Plots between experimental and calculated toxicity of CPs against (A) *D. magna*, (B) *B. rerio*, and (C) *Bacillus*.

Then, the training and test compounds are combined and the regression analysis is carried out on this combined data set (Table 8). Table 9 lists the observed and calculated values of log(1/LC_{50}) for CPs against *B. rerio*. Again, ω along with group philicities (ω_g^+ and ω_g^-) are capable of explaining maximum

Table 7. Regression Models for the Toxicity [log(1/LC_{50})] against *B. rerio* Using Various Descriptors for the Training Set of 16 CPs

s. no.	regression equation	r^2	r_{cv}^2	SD
1	$\log(1/LC_{50}) = -2.5 + 215.2 \times \omega_g^-$	0.557	0.438	0.348
2	$\log(1/LC_{50}) = -0.9 + 29.6 \times \omega$	0.721	0.637	0.281
3	$\log(1/LC_{50}) = -1.7 + 23.1 \times \omega + 69.9 \times \omega_g^-$	0.736	0.603	0.279
4	$\log(1/LC_{50}) = -4.1 - 0.8 \times \omega + 593.4 \times \omega_g^+$	0.906	0.851	0.166
5	$\log(1/LC_{50}) = -4.0 + 580.4 \times \omega_g^+$	0.906	0.881	0.160
6	$\log(1/LC_{50}) = -4.3 + 504.2 \times \omega_g^+ + 53.0 \times \omega_g^-$	0.924	0.892	0.150
7	$\log(1/LC_{50}) = -4.9 - 7.6 \times \omega + 595.1 \times \omega_g^+ + 71.4 \times \omega_g^-$	0.931	0.882	0.148

Table 8. Regression Models for the Toxicity [log(1/LC_{50})] against *B. rerio* Using Various Descriptors for the Data Set of 18 CPs

s. no.	regression equation	r^2	r_{cv}^2	SD
1	$\log(1/LC_{50}) = -2.5 + 212.3 \times \omega_g^-$	0.568	0.461	0.326
2	$\log(1/LC_{50}) = -0.8 + 29.3 \times \omega$	0.686	0.611	0.278
3	$\log(1/LC_{50}) = -1.9 + 21.1 \times \omega + 89.3 \times \omega_g^-$	0.733	0.612	0.265
4	$\log(1/LC_{50}) = -4.0 - 0.2 \times \omega + 583.5 \times \omega_g^+$	0.907	0.860	0.156
5	$\log(1/LC_{50}) = -4.0 + 580.7 \times \omega_g^+$	0.907	0.885	0.151
6	$\log(1/LC_{50}) = -4.3 + 503.8 \times \omega_g^+ + 51.4 \times \omega_g^-$	0.925	0.894	0.141
7	$\log(1/LC_{50}) = -4.6 - 4.3 \times \omega + 555.0 \times \omega_g^+ + 59.9 \times \omega_g^-$	0.928	0.878	0.143

Table 9. Experimental and Calculated Values of Toxicity [log(1/LC_{50})] against *B. rerio* for the Model Constructed Using the Data Set of 18 CPs

		log(1/LC_{50}) value (mmol/L)		
s. no.	molecule	experimental[a]	calculated[b]	residual[c]
1	2-MCP	0.93	0.87	0.06
2	3-MCP	0.92	1.14	−0.22
3	4-MCP	1.17	1.09	0.08
4	2,3-DCP	1.54	1.56	−0.02
5	2,4-DCP	1.54	1.63	−0.09
6	2,5-DCP	1.72	1.53	0.19
7	2,6-DCP	1.35	1.25	0.10
8	3,4-DCP	1.98	1.67	0.31
9	3,5-DCP	1.97	2.08	−0.11
10	2,3,4-TCP	2.01	1.99	0.02
11	2,3,5-TCP	2.14	2.20	−0.06
12	2,3,6-TCP	1.42	1.57	−0.15
13	2,4,5-TCP	2.17	2.08	0.09
14	2,4,6-TCP	1.89	1.91	−0.02
15	3,4,5-TCP	2.31	2.29	0.02
16	2,3,4,5-TTP	2.42	2.42	0.00
17	2,3,4,6-TTP		2.17[d]	
18	2,3,5,6-TTP	1.81	1.90	−0.09
19	PCP	2.53	2.39	0.14

[a] Experimental data as obtained from refs *23* and *24*. [b] With ω, ω_g^+, and ω_g^- as descriptors. [c] Difference between experimental and calculated toxicity values. [d] Predicted value using the developed model.

variation (92.8%) in data with a cross-validated squared correlation coefficient (r_{cv}^2) of 0.878 and a possibility of collinearity. A plot between observed and calculated values of log(1/LC_{50}) for CPs against *B. rerio* (Figure 3B) shows a correlation coefficient, *r*, of 0.964.

CP vs *Bacillus.* Table 10 presents the linear regression analyses carried out using experimental toxicity [log(1/IC_{50})] (*25*, *26*) against *Bacillus* as a dependent variable and various combinations of the selected descriptors as independent variables on the training set of 16 CPs. ω along with group philicities (ω_g^+ and ω_g^-) are capable of explaining maximum variation (93.6%) in data with a cross-validated squared correlation coefficient (r_{cv}^2) of 0.881. Hence, this QSAR model is used to predict the log(1/IC_{50}) values of molecules in the test set. That is, for 3,5-DCP (2,3,4-TCP), the observed log(1/IC_{50}) value is 0.81 (1.18) and the predicted value is 1.15 (0.82).

The training and test compounds are now combined, and the regression analysis is carried out on this combined data set (Table 11). Table 12 lists the observed and calculated values of log(1/IC_{50}) for CPs against *Bacillus*. Again, ω along with group philicities (ω_g^+ and ω_g^-) are capable of explaining maximum variation (91.9%) in data with a cross-validated squared correlation coefficient (r_{cv}^2) of 0.863. A plot between observed and calculated values of log(1/IC_{50}) for CPs against *Bacillus* (Figure 3C) shows a correlation coefficient, *r*, of 0.959.

A need now arises to evaluate and compare the performance of the method recently used in the establishment of QSAR for toxicity prediction of CPs against *D. magna*, *B. rerio*, and *Bacillus*. Brien et al. (*54*) have carried out a CATALYST study for a data set of 18 CPs and obtained a coefficient of determination, r^2, value of 0.832 (0.848, 0.857) with a standard error of estimation as 0.268 (0.193, 0.310) without reported values of cross-validation for *D. magna* (*B. rerio*, *Bacillus*). In the present study, using group philicities and/or electrophilicity

Table 10. Regression Models for the Toxicity [log(1/IC_{50})] against *Bacillus* Using Various Descriptors for the Training Set of 16 CPs

s. no.	regression equation	r^2	r_{cv}^2	SD
1	$\log(1/IC_{50}) = -5.5 + 299.7 \times \omega_g^-$	0.402	0.236	0.663
2	$\log(1/IC_{50}) = -3.56 + 45.0 \times \omega$	0.614	0.524	0.533
3	$\log(1/IC_{50}) = -4.0 + 41.4 \times \omega + 39.0 \times \omega_g^-$	0.617	0.435	0.551
4	$\log(1/IC_{50}) = -9.0 + 953.9 \times \omega_g^+$	0.910	0.886	0.257
5	$\log(1/IC_{50}) = -9.0 + 973.2 \times \omega_g^+ - 13.4 \times \omega_g^-$	0.911	0.858	0.266
6	$\log(1/IC_{50}) = -10.3 - 18.9 \times \omega + 1247.1 \times \omega_g^+$	0.933	0.894	0.231
7	$\log(1/IC_{50}) = -10.8 - 22.9 \times \omega + 1248.1 \times \omega_g^+ + 42.3 \times \omega_g^+$	0.936	0.881	0.234

Table 11. Regression Models for the Toxicity [log(1/IC_{50})] against *Bacillus* Using Various Descriptors for the Data Set of 18 CPs

s. no.	regression equation	r^2	r_{cv}^2	SD
1	$\log(1/IC_{50}) = -5.6 + 306.9 \times \omega_g^-$	0.428	0.293	0.625
2	$\log(1/IC_{50}) = -3.5 + 45.0 \times \omega$	0.584	0.495	0.533
3	$\log(1/IC_{50}) = -4.6 + 36.2 \times \omega + 95.2 \times \omega_g^-$	0.603	0.447	0.538
4	$\log(1/IC_{50}) = -9.1 + 966.5 \times \omega_g^+ - 1.8 \times \omega_g^-$	0.901	0.853	0.269
5	$\log(1/IC_{50}) = -9.1 + 963.7 \times \omega_g^+$	0.901	0.879	0.260
6	$\log(1/IC_{50}) = -10.1 - 15.1 \times \omega + 1191.3 \times \omega_g^+$	0.917	0.880	0.246
7	$\log(1/IC_{50}) = -10.4 - 17.4 \times \omega + 1175.6 \times \omega_g^+ + 32.9 \times \omega_g^-$	0.919	0.863	0.251

Table 12. Experimental and Calculated Values of Toxicity [log(1/IC$_{50}$)] against *Bacillus* for the Model Constructed Using the Data Set of 18 CPs

		log(1/IC$_{50}$) value (mmol/L)		
s. no.	molecule	experimental[a]	calculated[b]	residual[c]
1	2-MCP	−0.74	−1.11	0.37
2	3-MCP	−0.54	−0.44	−0.10
3	4-MCP	−0.49	−0.55	0.06
4	2,3-DCP	0.10	0.04	0.06
5	2,4-DCP	0.34	0.22	0.12
6	2,5-DCP	0.28	0.25	0.03
7	2,6-DCP	−0.53	−0.58	0.05
8	3,4-DCP	0.50	0.45	0.05
9	3,5-DCP	0.81	1.06	−0.25
10	2,3,4-TCP	1.18	0.78	0.40
11	2,3,5-TCP	1.30	1.29	0.01
12	2,3,6-TCP	0.02	0.20	−0.18
13	2,4,5-TCP	1.22	1.06	0.16
14	2,4,6-TCP	−0.08	0.51	−0.59
15	3,4,5-TCP	1.60	1.47	0.13
16	2,3,4,5-TTP	1.76	1.53	0.23
17	2,3,4,6-TTP		1.03[d]	
18	2,3,5,6-TTP	0.63	0.62	0.01
19	PCP	1.47	1.26	0.21

[a] Experimental data as obtained from refs *25* and *26*. [b] With ω, ω_g^+, and ω_g^- as descriptors. [c] Difference between experimental and calculated toxicity values. [d] Predicted value using the developed model.

as descriptors for the same data set of 18 CPs, we get a coefficient of determination, r^2, value of 0.889 (0.928, 0.919) with a standard error of estimation as 0.164 (0.143, 0.251) and internal predictive ability, r_{cv}^2, of 0.838 (0.878, 0.863) for *D. magna* (*B. rerio*, *Bacillus*). The models developed using the present approach and CATALYST study show the rising toxicity with the increasing degree of chlorination. It is well-known (*11*, *12*) that toxicity of CPs is reduced when chlorines substitute both ortho positions. This ortho effect is also well taken care of in the present study. For instance, among trichlorophenols (TCPs), 2,3,6-TCP and 2,4,6-TCP have the lowest toxicity values (Tables 6, 9, and 12), which is also true in the case of the CATALYST (*54*) approach. The above results clearly show the better performance of our selected descriptors in ecotoxicity prediction of CPs.

In summary, QSAR modeling is a useful technique to correlate physical, chemical, biological, or environmental activities of chemical species with their conceptual DFT-based descriptors. The application of group philicity in QSAR studies on ecotoxicology of CPs is one such effort that has been successfully tested for the first time. The combination of group philicities (ω_g^+ and ω_g^-) is capable of providing the highest correlation with good internal predictive ability and hence a good QSAR model for ecotoxicity of CPs against *D. magna*. Furthermore, electrophilicity along with group philicities (ω_g^+ and ω_g^-) are shown to provide reliable QSAR models having the highest coefficients of determination and internal predictive abilities for ecotoxicities of CPs against *B. rerio* and *Bacillus*. Comparison with a previous study reveals the satisfactory performance of the chosen descriptors. The above analysis clearly shows the importance of the selected descriptors in the QSAR analysis on the ecotoxicology of CPs.

Acknowledgment. We are thankful to CSIR, New Delhi, for financial assistance. J.P. thanks the UGC for selecting him to carry out his Ph.D. work under F.I.P.

References

(1) Verschueren, K. (1996) *Handbook of Environmental Data on Organic Chemicals*, 3rd ed., Van Nostrand Reinhold Company, New York.

(2) Della, G. M., Monaco, P., Pinto, G., Pollio, A., Previtera, L., and Temussi, F. (2001) Phytotoxicity of low-molecular-weight phenols from olive mill wastewaters. *Bull. Environ. Contam. Toxicol. 67*, 352−359.

(3) Garg, R., Kapur, S., and Hansch, C. (2001) Radical toxicity of phenols: a reference point for obtaining perspective in the formulation of QSAR. *Med. Res. Rev. 21*, 73−82.

(4) Giacalone, V. F. (1997) Phenol matrixectomy in patients with diabetes. *J. Foot Ankle Surg. 36*, 264−267.

(5) Dean-Ross, D., and Rahimi, M. (1995) Toxicity of phenolic compounds to sediment bacteria. *Bull. Environ. Contam. Toxicol. 55*, 245−250.

(6) Strotmann, U. J., and Eglsaer, H. (1995) The toxicity of substituted phenols in the nitrification inhibition test and luminescent bacteria test. *Ecotoxicol. Environ. Saf. 30*, 269−273.

(7) Gupta, V. K., and Ali, I. (2002) *Adsorbents for Water Treatment: Low Cost Alternatives to Carbon, Encyclopedia of Surface and Colloid Science* (Hubbard, A., Ed.) Vol. 1, pp 136−166, Marcel Dekker, New York.

(8) Zeeman, M., Auer, C. M., Clements, R. G., Nabholz, J. V., and Boethling, R. S. (1995) U.S. EPA regulatory perspectives on the use of QSAR for new and existing chemical evaluations. *SAR QSAR Environ. Res. 3*, 179−201.

(9) Briens, F., Bureau, R., Rault, S., and Robba, M. (1995) Applicability of CoMFA in ecotoxicology: A critical study on chlorophenols. *Ecotoxicol. Environ. Saf. 31*, 37−48.

(10) Bureau, R., Faucon, J. C., Faisant, J., Briens, F., and Rault, S. (1997) Applicability of the free energies of solvation for the prediction of ecotoxicity: Study of chlorophenols. *SAR QSAR Environ. Res. 6*, 163−181.

(11) Cohen, E., Gamliel, A., and Katan, J. (1988) The fungitoxicity of chlorophenols to the pathogenic fungi, *Fusarium oxysporum* and *Rhizoctonia solani*: A structure−activity relationship study. *Pestic. Sci. 24*, 139−146.

(12) Kishino, T., and Kobayashi, K. (1996) Acute toxicity and structure−activity relationships of chlorophenols in fish. *Water Res. 30*, 387−392.

(13) Chermette, H. (1999) Chemical reactivity indexes in density functional theory. *J. Comput. Chem. 20*, 129−154.

(14) Chattaraj, P. K., Nath, S., and Maiti, B. (2003) Reactivity descriptors. In *Computational Medicinal Chemistry for Drug Discovery* (Tollenaere, J., Bultinck, P., Winter, H. D., and Langenaeker, W., Eds.) Chapter 11, pp 295−322, Marcel Dekker, New York.

(15) Geerlings, P., De Proft, F., and Langenaeker, W. (2003) Conceptual density functional theory. *Chem. Rev. 103*, 1793−1874. (b) Chattaraj, P. K., Ed. (2005) Special issue on chemical reactivity. *J. Chem. Sci. 117*.

(16) Parthasarathi, R., Padmanabhan, J., Subramanian, V., Maiti, B., and Chattaraj, P. K. (2003) Chemical reactivity profiles of two selected polychlorinated biphenyls. *J. Phys. Chem. A 107*, 10346−10352.

(17) Parthasarathi, R., Padmanabhan, J., Subramanian, V., Sarkar, U., Maiti, B., and Chattaraj, P. K. (2003) Toxicity analysis of benzidine through chemical reactivity and selectivity profiles: A DFT approach. *Internet Electron J. Mol. Des. 2*, 798−813.

(18) Parthasarathi, R., Padmanabhan, J., Subramanian, V., Maiti, B., and Chattaraj, P. K. (2004) Toxicity analysis of 3′4′4′5-pentachloro biphenyl through chemical reactivity and selectivity profiles. *Curr. Sci. 86*, 535−542.

(19) Parthasarathi, R., Subramanian, V., Roy, D. R., and Chattaraj, P. K. (2004) Electrophilicity index as a possible descriptor of biological activity. *Bioorg. Med. Chem. 12*, 5533−5543.

(20) Roy, D. R., Parathasarathi, R., Maiti, B., Subramanian, V., and Chattaraj, P. K. (2005) Electrophilicity as a possible descriptor for toxicity prediction. *Bioorg. Med. Chem. 13*, 3405−3412.

(21) Padmanabhan, J., Parthasarathi, R., Subramanian, V., and Chattaraj, P. K. (2005) Chemical reactivity analysis on 3′4′4′5′-hexa chlorobiphenyl-A DFT approach. *J. Mol. Struct. (THEOCHEM) 730*, 221−226.

(22) Roy, D. R., Sarkar, U., Chattaraj, P. K., Mitra, A., Padmanabhan, J., Parthasarathi, R., Subramanian, V., Vandamme, S., and Bultinck, P. Analyzing toxicity through electrophilicity. *Mol. Diversity*, in press.

(23) Devillers, J., and Chambon, P. (1986) Acute toxicity and QSAR of chlorophenols on *Daphnia magna*. *Bull. Environ. Contam. Toxicol. 37*, 599−605.

(24) Devillers, J., and Chambon, P. (1986) Toxicité aiguë chlorophénols sur *Daphnia magna* et *Brachydanio rerio*. *J. Fr. Hydrol. 17*, 111−120.

(25) Liu, D., Thomson, K., and Kaiser, K. L. E. (1982) Quantitative structure-toxicity relationship of halogenated phenols on bacteria. *Bull. Environ. Contam. Toxicol. 29*, 130−136.

(26) Ribo, J. M., and Kaiser, J. L. E. (1983) Effects of selected chemicals to photoluminescent bacteria and their correlations with acute and sublethal effects on other organisms. *Chemosphere 12*, 1421−1442.

(27) Pearson, R. G. (1997) *Chemical Hardness—Applications from Molecules to Solids*, VCH−Wiley, Weinheim.
(28) Parr, R. G., and Yang, W. (1989) *Density Functional Theory of Atoms and Molecules*, Oxford University Press, Oxford.
(29) Iczkowski, R. P., and Margrave, J. L. (1961) Electronegativity. *J. Am. Chem. Soc. 83*, 3547−3551.
(30) Yang, W., and Mortier, W. J. (1986) The use of global and local molecular parameters for the analysis of the gas-phase basicity of amines. *J. Am. Chem. Soc. 108*, 5708−5711.
(31) Lee, C., Yang, W., and Parr, R. G. (1988) Local softness and chemical reactivity in the molecules CO, SCN^- and H_2CO. *J. Mol. Struct. (THEOCHEM) 163*, 305−313.
(32) Cioslowski, J., Martinov, M., and Mixon, S. T. (1993) Atomic Fukui indexes from the topological theory of atoms in molecules applied to Hartree−Fock and correlated electron densities. *J. Phys. Chem. 97*, 10948−10951.
(33) Parr, R. G., Szentpaly, L. V., and Liu, S. (1999) Electrophilicity Index. *J. Am. Chem. Soc. 121*, 1922−1924.
(34) Maynard, A. T., Huang, M., Rice, W. G., and Covell, D. G. (1998) Reactivity of the HIV-1 nucleocapsid protein p7 zinc finger domains from the perspective of density-functional theory. *Proc. Natl. Acad. Sci. U.S.A. 95*, 11578−11583.
(35) Chattaraj, P. K., Maiti, B., and Sarkar, U. (2003) Philicity: A unified treatment of chemical reactivity and selectivity. *J. Phys. Chem. A 107*, 4973−4975.
(36) Parthasarathi, R., Padmanabhan, J., Elango, M., Subramanian, V., and Chattaraj, P. K. (2004) Intermolecular reactivity through the generalized philicity concept. *Chem. Phys. Lett. 394*, 225−230.
(37) Parr, R. G., and Pearson, R. G. (1983) Absolute hardness: companion parameter to absolute electronegativity. *J. Am. Chem. Soc. 105*, 7512−7516.
(38) Chatterjee, S., Price, B., and Hadi, A. S. (1999) *Regression Analysis by Example. Wiley Series in Probability and Statistics*, 3rd ed., John Wiley & Sons, New York.
(39) Lucic, B., and Trinajstic, N. (1999) Multivariate regression outperforms several robust architectures of neural networks in QSAR modeling. *J. Chem. Inf. Comput. Sci. 39*, 121−132.
(40) Becke, A. D. (1998) Density-functional exchange-energy approximation with correct asymptotic behavior. *Phys. Rev. A 38*, 3098−3100.
(41) Lee, C., Yang, W., and Parr, R. G. (1988) Development of the Colle-Salvetti correlation-energy formula into a functional of the electron density. *Phys. Rev. B 37*, 785−789.
(42) Hariharan, P. C., and Pople, J. A. (1973) The influence of polarization functions on molecular orbital hydrogenation energies. *Theor. Chim. Acta. 28*, 213−222.
(43) Frisch, M. J., Trucks, G. W., Schlegel, H. B., Scuseria, G. E., Robb, M. A., Cheeseman, J. R., Zakrzewski, V. G., Montgomery, J. A., Jr., Stratmann, R. E., Burant, J. C., Dapprich, S., Millam, J. M., Daniels, A. D., Kudin, K. N., Strain, M. C., Farkas, O., Tomasi, J., Barone, V., Cossi, M., Cammi, R., Mennucci, B., Pomelli, C., Adamo, C., Clifford, S., Ochterski, J., Petersson, G. A., Ayala, P. Y., Cui, Q., Morokuma, K., Malick, D. K., Rabuck, A. D., Raghavachari, K., Foresman, J. B., Cioslowski, J., Ortiz, J. V., Stefanov, B. B., Liu, G., Liashenko, A., Piskorz, P., Komaromi, I., Gomperts, R., Martin, R. L., Fox, D. J., Keith, T., Al-Laham, M. A., Peng, C. Y., Nanayakkara, A., Gonzalez, C., Challacombe, M., Gill, P. M. W., Johnson, B. G., Chen, W., Wong, M. W., Andres, J. L., Head-Gordon, M., Replogle, E. S., and Pople, J. A. (1998) *Gaussian 98*, revision A.7, Gaussian, Inc., Pittsburgh, PA.
(44) Hirshfeld, F. L. (1977) Bonded-atom fragments for describing molecular charge densities. *Theor. Chim. Acta 44*, 129−138.
(45) DMOL[3], Accelrys, Inc., San Diego, California.
(46) *MATLAB* (1999) The Math Works, Inc., Natick, United States.
(47) Penrose, R. (1955) A generalized inverse for matrices. *Proc. Camb. Philos. Soc. 51*, 406−413.
(48) Ishizaki, K., Larson, T. R., Schauer, N., Fernie, A. R., Graham, I. A., and Leaver, C. J. (2005) The critical role of *Arabidopsis* electron-transfer flavoprotein: Ubiquinone oxidoreductase during dark-induced starvation. *Plant Cell 17*, 2587−2600 and references therein.
(49) Dai, J., Wright, M. W., and Manderville, R. A. (2003) An oxygen-bonded C8-deoxyguanosine nucleoside adduct of pentachlorophenol by peroxidase activation: Evidence for ambident C8 reactivity by phenoxyl radicals. *Chem. Res. Toxicol. 16*, 817−821.
(50) Dai, J., Sloat, A. L., Wright, M. W., and Manderville, R. A. (2005) Role of phenoxyl radicals in DNA adduction by chlorophenol xenobiotics following peroxidase activation. *Chem. Res. Toxicol. 18*, 771−779.
(51) Aschmann, C., Stork, T., and Wassermann, O. (1989) Short-term effects of chlorophenols on the function and viability of primary cultured rat hepatocytes. *Arch. Toxicol. 63*, 121−126.
(52) van Ommen, B., Adang, A., Muller, F., and van Bladeren, P. J. (1986) The microsomal metabolism of pentachlorophenol and its covalent binding to protein and DNA. *Chem.-Biol. Interact. 60*, 1−11.
(53) Chin-Hsiang, T., Po-Hsiung, L., Troester, M. A., and Rappaport, S. M. (2003) Formation and removal of pentachlorophenol-derived protein adducts in rodent liver under acute, multiple, and chronic dosing regimens. *Toxicol. Sci. 73*, 26−35.
(54) Briens, F., Bureau, R., and Rault, S. (1999) Applicability of CATALYST in ecotoxicology, a new promising tool for 3D-QSAR: Study of chlorophenols. *Ecotoxicol. Environ. Saf. 43*, 241−251.

TX050322M